AJNR

Vascular characteristics of intracerebral arteriovenous malformations in patients with clinical steal.

M P Marks, B Lane, G Steinberg and P Chang

AJNR Am J Neuroradiol 1991, 12 (3) 489-496
http://www.ajnr.org/content/12/3/489

Vascular Characteristics of Intracerebral Arteriovenous Malformations in Patients with Clinical Steal

Michael P. Marks[1]
Barton Lane[1]
Gary Steinberg[2]
Paul Chang[1]

In patients with intracerebral arteriovenous malformations (AVMs), symptoms attributed to steal can lead to progressive debilitating deficits. This study was undertaken to determine which morphologic features of the AVM could be correlated with clinical symptoms of steal. Over a 4-year period, 65 patients with intracranial AVMs were evaluated with angiography supplemented by MR (46 cases) and CT (19 cases). Eleven characteristics of AVM vascular architecture were studied; these included size, lobar location, periventricular/intraventricular location, arterial stenosis, arteriovenous fistulae, angiomatous change (the presence of dilated transcortical collateral circulation), venous drainage pattern (central, cortical, mixed), venous stenosis, venous aneurysm or ectasia, venous variation, and delayed drainage. These characteristics were correlated with a history of clinical steal, which was seen in nine (14%) of 65 patients. Three characteristics were found to correlate highly with steal: angiomatous change ($p < .0001$), size ($p < .0001$), and peripheral venous drainage ($p = .045$). The mean size of the AVM nidus was 31.3 cm^3 for the entire group of patients, 105.0 cm^3 for patients with steal, and 19.5 cm^3 for those without steal symptoms. Angiomatous change was seen in six (9%) of 65 patients; all six of these had clinical steal.

The association of clinical steal with AVM size, angiomatous change, and peripheral venous drainage may contribute to establishing a prognosis and treatment planning. When a patient's symptoms are caused by steal, treatment with subtotal excision or partial embolization may be beneficial.

***AJNR* 12:489–496, May/June 1991**

Arteriovenous malformations (AVMs) found in the brain are congenital vascular malformations that result in direct arteriovenous shunts [1]. Patients with AVMs present with a variety of symptoms, including seizures, headaches, hemorrhage, progressive neurologic deficits, and intellectual deterioration. Gradually progressive neurologic deficits (often with a stuttering course) and intellectual deterioration have been attributed to stealing of blood by the malformation [2, 3]. The phenomenon of steal occurs when arterial blood is shunted through the low-resistance arteriovenous fistulae of the AVM away from the higher-resistance capillary bed in the normal brain adjacent to the AVM [4]. Blood flow to the normal surrounding brain gradually decreases with time and eventually reaches the point at which perfusion is inadequate to maintain normal neuronal electric activity, approximately 15–18 $ml \cdot 100\ g\ brain^{-1} \cdot min^{-1}$ [4, 5].

It is difficult to prove that hypoperfusion due to steal is the cause of a patient's symptoms. Various techniques have been used to evaluate flow-related changes in the parenchyma surrounding the AVM. These have included radionuclide cerebral blood flow determinations, single-photon emission CT (SPECT), stable xenon CT, and IV dynamic CT [6–10]. While these techniques have all shown changes in cerebral blood flow in the surrounding parenchyma, they have not been able to determine absolute values of flow reduction to account for symptoms of clinical steal.

Received May 29, 1990; revision requested August 10, 1990; revision received December 6, 1990; accepted December 7, 1990.

[1] Department of Diagnostic Radiology, Room S072, Stanford University Medical Center, Stanford, CA 94305. Address reprint requests to M. P. Marks.

[2] Department of Neurosurgery, Stanford University Medical Center, Stanford, CA 94305.

0195-6108/91/1203-0489

This study was undertaken to evaluate a commonly used technique (angiography supplemented by either CT or MR) in order to identify AVM characteristics that may predispose to clinical steal symptoms in patients with intracerebral AVMs.

Materials and Methods

We retrospectively evaluated the angiograms, CT scans, and MR images of 65 patients with intracranial AVMs seen at our institution over a 4-year period. The same group was recently evaluated in a retrospective study of vascular characteristics associated with hemorrhage [11]. The study group comprised 31 males and 34 females 9–69 years old (mean, 33 years). Clinical history was obtained from review of the hospital charts or records in the division of neurosurgery. Patients presenting with gradual, progressive neurologic symptoms were judged to have steal. Their symptoms were not considered to be due to steal if a single ictus (on the basis of stroke) or a series of discrete individual events had led to a portion of their disability. Patients with inadequate history were eliminated from the study, as were patients with prior neurosurgical or endovascular procedures.

All patients had selective carotid and vertebral biplane angiography, which was used to evaluate most of the vascular characteristics. Many of the angiograms were filmed as simultaneous biplane studies and usually filmed at a sequence of two films per second for 3 sec, one film per second for 3 sec, and one film every other second for 4–6 sec. In those lesions with higher flow rates, filming was performed in a single plane at up to four films per second. CT (19 cases) or MR (46 cases) studies were also performed at the time of angiography. CT was performed on a GE 9800 scanner (General Electric, Milwaukee, WI) with 5-mm contiguous axial cuts through the posterior fossa and 10-mm axial cuts through the supratentorial brain. CT scans were obtained before and after enhancement. MR was done with a 1.5-T GE superconducting magnet. Routine spin-echo pulse sequences were obtained using T1-weighted images, 600/20 (TR/TE), in the sagittal and coronal planes. In addition, T2-weighted images, 2000/20, 80, were obtained in the axial plane. CT and MR were used predominantly to assist in the evaluation of location. They were also used to determine if infarction or significant gliosis was present. Gliosis is almost always found histologically interspersed between the vessels of the nidus [12]. Infarction or significant gliosis was judged to be present only when brain parenchyma beyond the margins of the nidus showed evidence of prior insult. Surrounding infarction or gliosis was determined on CT as areas of low attenuation. On MR, gliosis or infarction was seen as low signal intensity on T1-weighted images and high signal intensity on T2-weighted images.

Eleven vascular characteristics were evaluated for each patient. These characteristics were chosen because it was believed they could affect the hemodynamic status of the AVM and the surrounding brain. The characteristics evaluated were size, lobar location, periventricular/intraventricular location, arterial stenosis, arteriovenous fistula, angiomatous change, venous drainage (central, peripheral, or mixed), venous stenosis, venous aneurysm or ectasia, venous variation, and delayed drainage. Other morphologic characteristics such as saccular arterial aneurysms were not included because they were not thought to affect the hemodynamics of the AVM and surrounding brain.

Size was determined by a previously described volumetric method [13]. The size of the AVM nidus was measured in three planes (antero-posterior, mediolateral, and craniocaudal), and these measurements were multiplied to determine the volume of the AVM. Lobar location refers to the region occupied by the nidus (e.g., frontal, parietal, occipital). The center of the AVM nidus was used to determine the geographic location when the nidus was large and occupied more than one region of the brain. In addition, the AVM nidus was evaluated for a periventricular or intraventricular location. This meant that the nidus occupied a wall of the ventricle or was within the ventricle. This characteristic was determined by CT or MR. Arterial stenosis was judged to be present when a greater than 50% narrowing was demonstrated in an intracerebral artery supplying the AVM. Arteriovenous fistulae were recorded only when a direct arteriovenous communication could be determined early in the angiogram. Angiomatous change represented the presence of anomalous arterial blood supply to the AVM nidus. Usually this was seen to take the form of dilated transcortical or leptomeningeal arteries acting as collateral blood supply to the nidus. However, in at least one instance the angiomatous vessels were dilated basal perforating arteries providing collateral supply to the AVM.

Venous drainage referred to the pattern of central, cortical, or mixed (central and cortical) drainage. Venous stenosis was generally seen at the junction of major draining veins. This was most often present where the major vein entered a region of the dural sinus (such as the junction of the vein of Galen and straight sinus). It was judged to be present when there was a decrease in the venous diameter of greater than 50%. Venous ectasia or aneurysm was scored when a portion of the venous drainage system appeared markedly ectatic or had the appearance of a fusiform aneurysm. Venous variation referred to unexpected drainage given the location of the AVM nidus.

The vascular characteristics were all subjected to statistical analysis when correlated with the presence or absence of clinical steal. For continuous quantitative vascular characteristics (such as size), a two-sample, two-sided t test was used. The Fisher-Irwin Exact Test [14] was used for nominal qualitative characteristics (such as the presence or absence of arterial stenosis).

Results

Table 1 shows the clinical symptoms for the entire group of 65 patients evaluated. Nine (14%) of 65 patients had a history of gradual progressive neurologic deficits, which were representative of clinical steal. Seven (78%) of nine patients had gradual motor weakness and three (33%) of nine had gradual memory and/or cognitive impairment. The steal symptoms and additional clinical presentations of these nine patients are shown in Table 2. Three (33%) of nine patients had clinical episodes of ictus suggestive of prior hemorrhage. In two patients (cases 2 and 3), the ictus was more recent (less than 1 year old) and appeared to occur well after the onset of progressive deficits. The episodes of hemorrhage were documented in these two patients by CT scans at outside institutions. The hemorrhages did not worsen the patients' clinical deficit. One patient (case 4) had an episode suggestive of hemorrhage with loss of consciousness and a severe

TABLE 1: Clinical Symptoms in Patients with Arteriovenous Malformation

Symptom	No. (%) (n = 65)
Intracranial hemorrhage	45 (69)
Seizures	18 (28)
Headache	13 (20)
Migraine headache	10 (15)
Progressive neurologic deficit	9 (14)

Note.—Some patients had more than one symptom.

TABLE 2: Clinical Characteristics and Location and Size of Arteriovenous Malformations in Patients with Clinical Steal

Case No.	Age (yr)	Sex	Location (Side)	Size (cm^3)	Gradually Progressive Symptoms	Duration of Progressive Symptoms (yr)	Additional Symptoms
1	49	M	Frontal (R)	216	L-sided weakness	20	Bifrontal HA, seizures
2	11	M	Basal ganglia (L)	29	R-sided weakness, numbness	3	Hemorrhage
3	21	M	Basal ganglia (R)	70	L-sided weakness, memory loss	3	Hemorrhage
4	25	F	Cerebellar peduncle (L)	6	Ataxia, L facial weakness	1	HA, probable hemorrhage[a]
5	14	F	Frontal (L)	144	R-sided weakness	6	Migraine HA
6	36	M	Parietal (L)	288	Decreased intellectual function, memory loss	5	Seizure
7	43	F	Parietal (R)	125	L leg weakness	11	Seizure
8	43	F	Frontal (L)	31	Aphasia, memory loss	5	Seizure, migraine HA
9	20	M	Basal ganglia (L)	108	R-sided weakness	4	None

Note.—R = right, L = left, HA = headache.
[a] See text.

headache that occurred approximately 1 year before presentation at our hospital. This was not documented with imaging or lumbar puncture, however. This episode was not associated with a neurologic deficit and it predated the gradual deficits experienced by this patient. In none of the other patients were there any episodes suggestive of hemorrhage or stroke.

Lobar location was not found to be significant in those patients with clinical steal. For the entire study group the locations included frontal (11 patients), basal ganglia (10), parietal (nine), temporal (eight), thalamus (eight), brainstem (six), cerebellar (four), intraventricular (four), corpus callosum (three), and occipital (two).

Size was found to correlate highly with symptoms of clinical steal, with larger lesions predominating in the steal patients ($p < .0001$, two-sample t test). For the entire group of patients the size range was 0.33–288 cm^3 (mean, 31.3 cm^3; SEM, 6.3 cm^3). When steal was present, the range was 5.7–288 cm^3 (mean, 105 cm^3; SEM, 31.3 cm^3). In the group without steal the range was 0.33–160 cm^3 (mean, 19.5 cm^3; SEM, 3.7 cm^3).

Table 3 lists additional vascular characteristics, which were evaluated with the results for the entire study group and the results for patients with clinical steal. Angiomatous change correlated highly with clinical steal symptoms ($p < .0001$, Fisher-Irwin Exact Test). Angiomatous change was identified in six (9%) of 65 patients. All six of these patients had evidence of clinical steal, so that angiomatous change was seen in six (67%) of the nine patients with steal. Examples of patients with angiomatous change are shown in Figures 1 and 2. Figure 3 illustrates the relationship proposed between the AVM nidus and vessels representing angiomatous change. Peripheral venous drainage was also found to correlate with steal symptoms ($p = .045$, Fisher-Irwin Exact Test). Peripheral or cortical venous drainage was seen in five (56%) of nine patients. No other vascular characteristic was found to correlate with symptoms of clinical steal.

In all patients, either MR or CT was performed at our institution at the time of angiography. In the group of patients with steal symptoms, six had MR studies and three had CT studies. In one of the nine steal patients (case 4), these studies provided evidence of surrounding parenchymal change indicating infarction or gliosis (Fig. 4). Four (7%) of the 56 patients without steal had surrounding parenchymal gliosis.

TABLE 3: Vascular Characteristics in All Patients with Arteriovenous Malformation and in Those with Clinical Steal

Vascular Characteristic	No. of Patients (%)	
	Total Group ($n = 65$)	With Clinical Steal ($n = 9$)
Periventricular/intraventricular location	24 (37)	3 (33)
Arterial stenoses	3 (5)	2 (22)
Angiomatous change	6 (9)	6 (67)
Arteriovenous fistula	0	0
Venous drainage		
Central	34 (52)	3 (33)
Peripheral	19 (29)	5 (56)
Mixed	12 (19)	1 (11)
Venous stenosis	23 (36)	1 (11)
Venous ectasia	22 (34)	3 (33)
Venous variation	19 (29)	2 (22)
Delayed drainage	4 (6)	0

Discussion

This study has evaluated vascular characteristics of AVMs (seen predominantly at angiography) that may correlate highly with clinical symptoms of steal. When using radioisotope studies, Feindel and Perot [15] coined the term *cerebral steal* to describe vascular shunting seen with reduced circulation in surrounding cortex. Angiography has been used to describe *angiographic steal*, which can be seen with many AVMs. This should be differentiated from *clinical steal* symptoms, which may be seen in AVM patients. Clinical steal manifests as a progressive neurologic deterioration that can cause progressive focal neurologic deficits or changes in intellectual function. Occasionally, resection or embolization has been reported to improve these symptoms [3, 4].

Angiographic steal refers to the lack of opacification of vessels surrounding the AVM. Several authors have noted that opacification improved in vessels around an AVM after surgical resection [16–18]. Angiographic steal may be observed in patients with no evidence of clinical steal. The degree of opacification of blood vessels surrounding an AVM is dependent on many unrelated factors. Lack of filling of

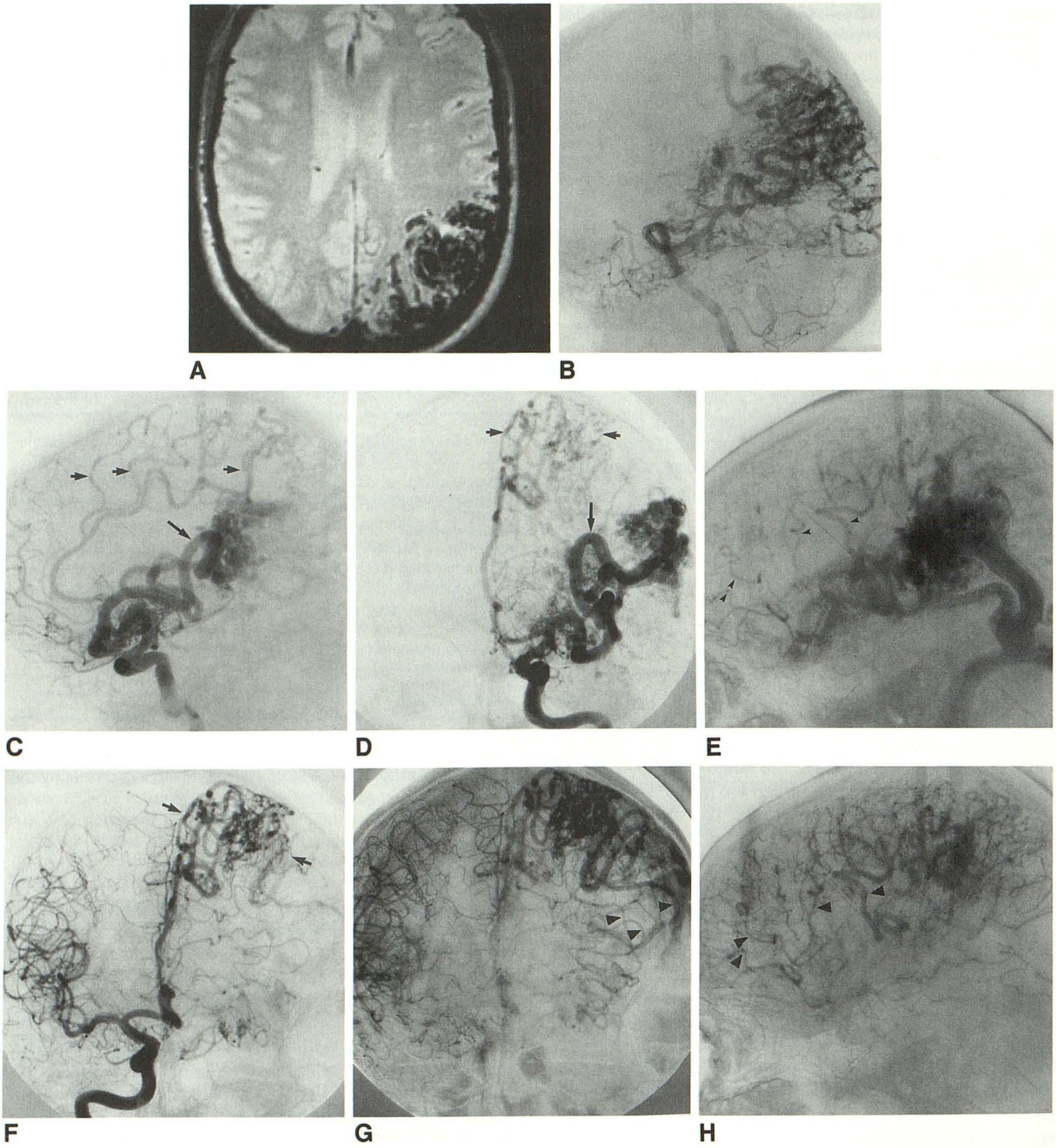

Fig. 1.—Case 6: 36-year-old man with left parietal arteriovenous malformation (AVM).

A, Axial MR image (2000/20) shows posterior parietal AVM.

B, Left vertebral angiogram, lateral projection. Dilated left posterior cerebral artery supplies AVM nidus.

C–E, Left internal carotid angiograms, lateral (*C* and *E*) and posteroanterior (*D*) projections, arterial (*C* and *D*) and lateral venous (*E*) phases. AVM is supplied directly by branches of middle cerebral artery (predominantly angular artery [*large arrows*]). There is poor filling of distal opercular vessels in arterial phase (*C* and *D*). On arterial-phase films, note dilated vessels of anterior cerebral artery territory (*C, small arrows*). These vessels supply a region of dilated cortical vessels that have undergone angiomatous change (best seen on *D*, area between *small arrows*). Region of angiomatous change then supplies opercular vessels, which filled late and in a retrograde fashion (*arrowheads*). The most posterior opercular vessel in *E* is noted to be dilated as it supplies AVM in a retrograde manner.

F–H, Right internal carotid angiogram, early arterial (*F*) and late arterial (*G* and *H*) phases. There is cross filling to left anterior cerebral circulation. Again note dilated appearance of vessels in this territory that have undergone angiomatous change (area between *arrows*) and compare them with right anterior cerebral circulation. Again noted is retrograde filling of distal opercular vessels on late arterial phase, including larger, more posterior opercular vessel (*arrowheads*).

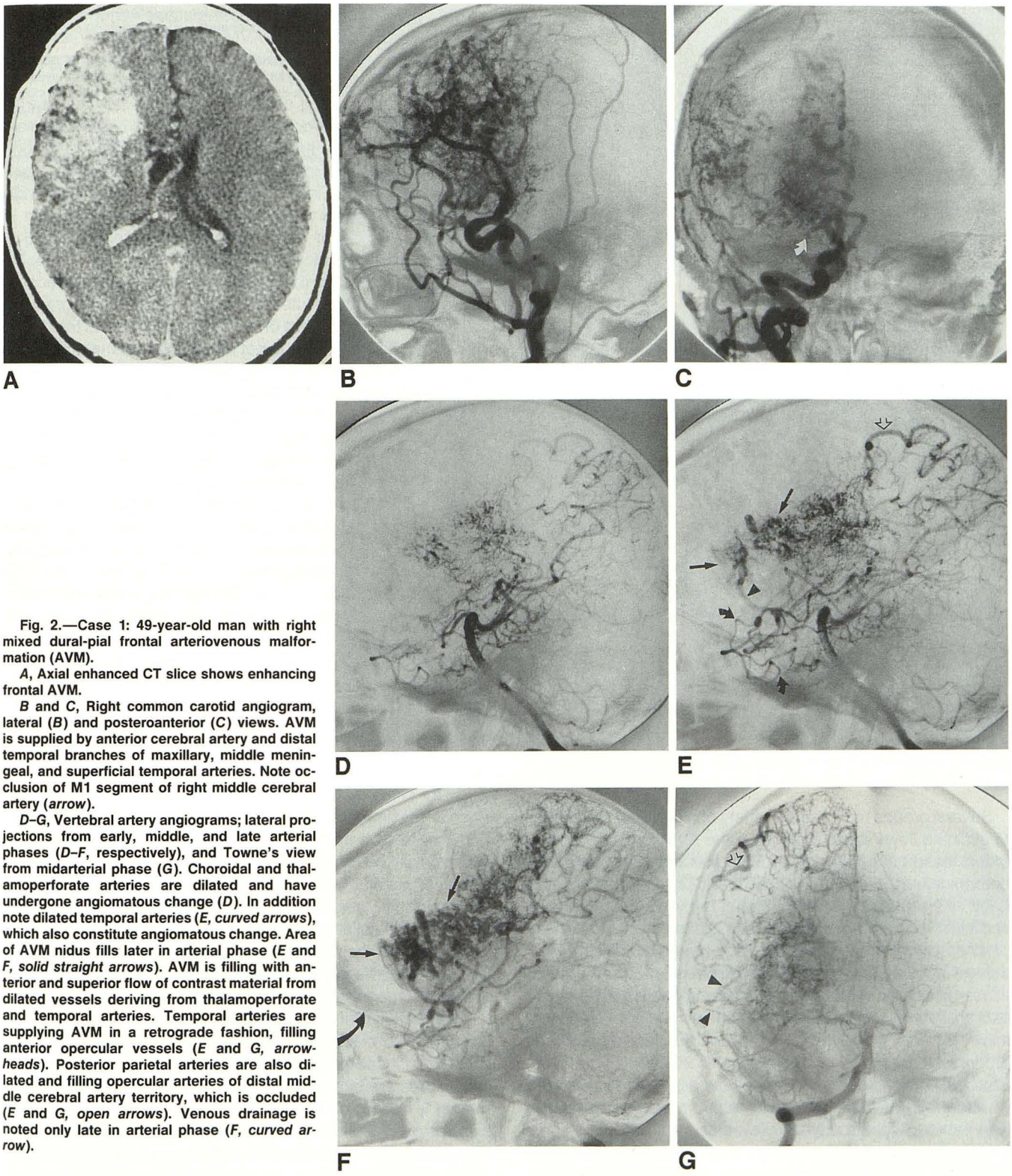

Fig. 2.—Case 1: 49-year-old man with right mixed dural-pial frontal arteriovenous malformation (AVM).

***A*, Axial enhanced CT slice shows enhancing frontal AVM.**

***B* and *C*, Right common carotid angiogram, lateral (*B*) and posteroanterior (*C*) views. AVM is supplied by anterior cerebral artery and distal temporal branches of maxillary, middle meningeal, and superficial temporal arteries. Note occlusion of M1 segment of right middle cerebral artery (*arrow*).**

***D–G*, Vertebral artery angiograms; lateral projections from early, middle, and late arterial phases (*D–F*, respectively), and Towne's view from midarterial phase (*G*). Choroidal and thalamoperforate arteries are dilated and have undergone angiomatous change (*D*). In addition note dilated temporal arteries (*E, curved arrows*), which also constitute angiomatous change. Area of AVM nidus fills later in arterial phase (*E* and *F, solid straight arrows*). AVM is filling with anterior and superior flow of contrast material from dilated vessels deriving from thalamoperforate and temporal arteries. Temporal arteries are supplying AVM in a retrograde fashion, filling anterior opercular vessels (*E* and *G, arrowheads*). Posterior parietal arteries are also dilated and filling opercular arteries of distal middle cerebral artery territory, which is occluded (*E* and *G, open arrows*). Venous drainage is noted only late in arterial phase (*F, curved arrow*).**

these arteries during angiography does not necessarily mean that perfusion to these portions of brain is reduced to a level that would cause clinical symptoms. Factors affecting opacification of intracerebral arteries in the vicinity of an AVM include the amount of contrast material injected, the speed of bolus injection, the vessel injected (e.g., common carotid vs internal carotid artery), and the degree of washout of contrast material from the anastomotic supply within the brain (e.g., posterior cerebral artery circulation may be supplied via the carotid artery and basilar artery).

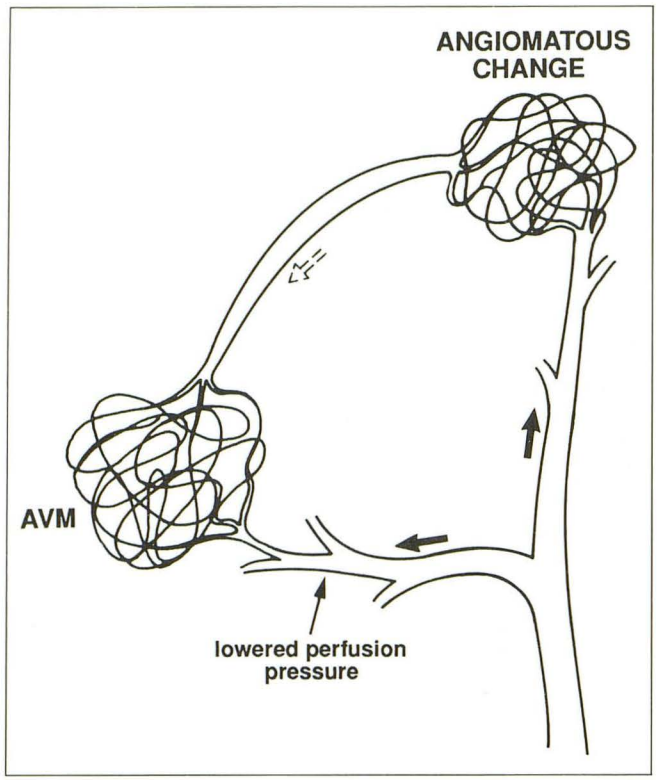

Fig. 3.—Illustration shows additional collateral arterial supply to arteriovenous malformation (AVM) from a vascular territory that has undergone angiomatous change. In this case, AVM nidus is supplied by transcortical or leptomeningeal collaterals. Proposed mechanism for development of these collaterals is that, despite maximum dilatation of arteries usually supplying AVM nidus, blood flow is inadequate to maintain perfusion pressures to nidus and parenchyma immediately around AVM. This results in recruitment of leptomeningeal collaterals, which causes these vessels to dilate, giving them an appearance similar to primary AVM nidus or angioma, and for this reason it has been termed angiomatous change.

Several groups have used a variety of blood flow techniques to evaluate flow-related changes in the AVM and surrounding brain; these have included radionuclide cerebral blood flow determinations [6, 19–21], SPECT [8, 22, 23], stable xenon CT [7, 10], and IV dynamic CT [9]. These methods have all shown some degree of decreased blood flow to the brain parenchyma around the AVM. They have not been able to definitively identify regions where flow was low enough to cause disturbances in neuronal electrical activity that would explain steal symptoms (approximately 15–18 $ml \cdot 100\ g^{-1} \cdot min^{-1}$) [5]. Batjer et al. [23] have recently correlated gradually progressive neurologic symptoms with SPECT flow studies. Statistically significant decreased flow adjacent to the AVM was found in patients with steal symptoms when compared with patients without steal.

The two angiographic findings that were associated with symptoms of steal in this series were size and the presence of angiomatous change. AVMs with a larger nidus are likely to cause a larger shunt burden to the existing cerebral vasculature and therefore are more likely to produce symptoms of steal. A significant positive correlation between larger AVM size and decreased flow in the cortical regions adjacent to an AVM has been reported when using stable xenon CT [10]. It is also possible that a large AVM could produce a neurologic deficit by virtue of an increased mass effect with compression of surrounding brain parenchyma.

Angiomatous change appears angiographically as a series of dilated vessels that supply the AVM nidus collaterally from arteries not normally expected to supply that AVM territory. In most cases these dilated collaterals are cortical or leptomeningeal vessels (Fig. 1), but in at least one case they were dilated perforating arteries similar to the collaterals seen in occlusions that occur with moyamoya disease. At angiography, this network of dilated vessels often has a tangled appearance similar to that of the AVM nidus, and because it looks like the angioma itself we have termed it angiomatous change. Closer inspection of the angiogram reveals that these dilated collateral vessels do not shunt contrast material to the venous side early in the angiogram like arteries of the AVM do. Instead, they exhibit slower circulation and demonstrate venous filling much later during angiography. These dilated vessels usually supply the AVM nidus via retrograde flow.

We believe these vessels represent collaterals and not angiogenic change. Pathologic studies have demonstrated arterial anastomoses at the cortical level in the human brain [24]. Angiographic demonstration of collateral supply beyond the circle of Willis in response to proximal occlusions has been described by several authors [25–27]. One of the main routes for this supply is via dilated cortical or leptomeningeal vessels shunting blood in a transcortical direction to supply the ischemic area in a retrograde fashion [25, 26]. An AVM is composed of altered arterioles that shunt blood directly to venous channels bypassing the normal higher-resistance capillary bed [4]. These arterioles have lost the ability to autoregulate, making the AVM a passive vascular system whereby blood flow is pressure dependent [28, 29]. Therefore, AVMs with lower perfusion pressures will have lower rates of flow [29]. In some AVMs, perfusion pressure will remain low despite maximal dilatation of the local arterial supply and the AVM will recruit supply from other vessels. These recruited vessels may come via transcortical supply and appear angiographically as angiomatous change. This may explain why angiomatous change is seen in patients with steal symptoms. Transcortical collaterals occur when there are low perfusion pressures to the AVM; these low pressures may reflect decreased perfusion in the brain immediately adjacent to the AVM. We have previously shown that angiomatous change is negatively correlated with hemorrhage, having a protective effect against bleeding [11]. Hemorrhage may be significantly reduced in those patients with angiomatous change because their AVMs are exposed to states of lowered perfusion pressures.

Large-vessel stenosis or occlusions have been described in an experimental model of high flow states [30] and in patients with AVMs [31, 32]. In two of the steal patients in our series, proximal arterial stenoses or occlusions were demonstrated in addition to angiomatous change. This would account for lowered perfusion pressure and the development of angiomatous change in these patients.

There are reasons for neurologic deficits in AVM patients

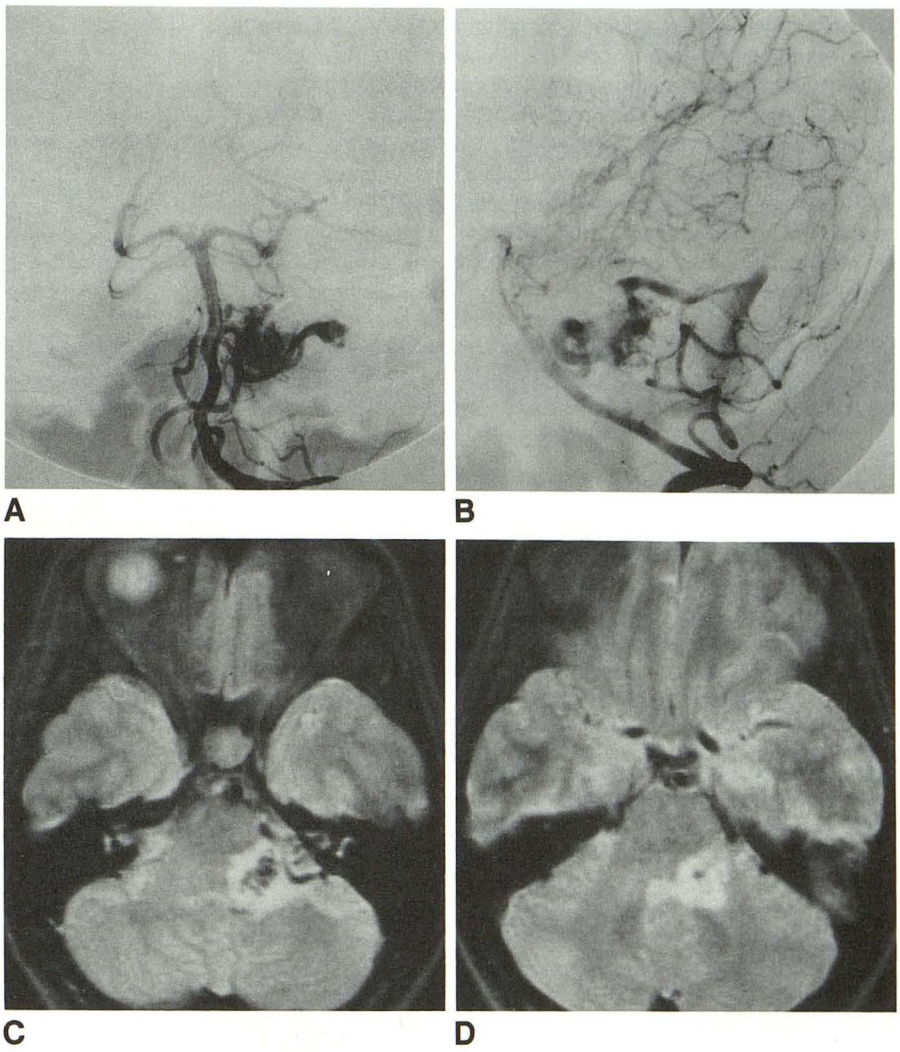

Fig. 4.—Case 4: 25-year-old woman with left cerebellar peduncle arteriovenous malformation (AVM).

***A* and *B*, Towne's and lateral views from a left vertebral angiogram show AVM nidus supplied predominantly by left anterior inferior cerebellar artery.**

***C* and *D*, Axial T2-weighted MR images show lower-signal flow voids of AVM nidus with a surrounding margin of high-signal gliotic tissue (*C*). On higher slice, a significant amount of gliosis is noted also in cerebellar peduncle (*D*).**

other than steal. The most likely cause is hemorrhage leading to a deficit [2]. We controlled for this by excluding patients in whom an episode of ictus led to a neurologic deficit. Three patients with steal symptoms had a clinical event thought to be a hemorrhage, but an associated neurologic deficit did not develop at the time of hemorrhage. Progressive neurologic symptoms may be due to multiple subclinical hemorrhages in a critical or eloquent region of the brain, such as has been reported in patients with brainstem vascular malformations [33]. None of the patients with steal symptoms in this study had brainstem lesions. However, one patient in this series (case 4) had a lesion in a critical region (the cerebellar peduncle), and it is possible that in this patient steal symptoms could have been due to multiple subclinical hemorrhages. MR did not show evidence of significant hemosiderin staining (Fig. 4), making multiple hemorrhages less likely.

CT and MR can assist in the evaluation of the AVM patient with clinical steal. They provide information regarding the surrounding parenchyma. Both MR and CT are able to show areas of surrounding infarction or gliosis. MR may indicate there has been a prior hemorrhagic event by demonstrating hemosiderin staining in the surrounding parenchyma.

The observation that peripheral venous drainage is highly correlated with steal symptoms is more difficult to explain on a hemodynamic basis. A prior study comparing venous drainage patterns and hemorrhage showed that central venous drainage correlated positively with a history of bleeding, while peripheral venous drainage correlated negatively with prior bleeding [11]. Therefore, our selection criteria, which eliminated patients with hemorrhage that contributed to their neurologic deficits (i.e., patients with central venous drainage), may have preferentially selected patients with peripheral venous drainage. It is also possible that cortically located AVMs are more likely to produce symptomatic steal, and peripheral venous drainage reflects this location.

In conclusion, we evaluated 11 vascular characteristics of AVMs and found that three correlated highly with clinical steal: larger size, angiomatous change, and peripheral venous drainage. The correlation of large size and angiomatous change with symptoms of steal can be explained on a hemo-

dynamic basis. These findings contribute additional information regarding the prognosis of the AVM patient. In addition, they may influence treatment planning. It is more difficult to achieve complete thrombosis or complete excision of these larger lesions. However, if a patient's symptoms are due to steal phenomenon it may be beneficial to treat such a lesion with subtotal excision or partial embolization. Data such as these may help to identify those patients with symptoms due to steal who would benefit from reduction of blood flow through their shunt vessels.

REFERENCES

1. Stein BM, Wolpert SM. Arteriovenous malformations of the brain. *Arch Neurol* **1980**;37:1–5
2. Luessenhop AJ. Natural history of cerebral arteriovenous malformations. In: Wilson CB, Stein BM, eds. *Intracranial arteriovenous malformations*, 1st ed. Baltimore: Williams & Wilkins, **1984**:12–23
3. Kusske JA, Kelly WA. Embolization and reduction of the "steal" syndrome in cerebral arteriovenous malformations. *J Neurosurg* **1974**;40:313–321
4. Spetzler RF, Selman WR. Pathophysiology of cerebral ischemia accompanying arteriovenous malformations. In: Wilson CB, Stein BM, eds. *Intracranial arteriovenous malformations*, 1st ed. Baltimore: Williams & Wilkins, **1984**:24–31
5. Meyer FB, Sundt TM, Yanagihara T, Anderson RE. Focal cerebral ischemia: pathophysiologic mechanisms and rationale for future avenues of treatment. *Mayo Clin Proc* **1987**;62:35–55
6. Feindel W, Yamamoto YL, Hodge CP. Red cerebral veins and the cerebral steal syndrome. *J Neurosurg* **1971**;35:167–179
7. Okabe T, Meyer JS, Okayasu H, et al. Xenon-enhanced CT CBF measurements in cerebral AVMs before and after excision. *J Neurosurg* **1983**;59:21–31
8. Takeuchi S, Kikuchi H, Karasawa J, et al. Cerebral hemodynamics in arteriovenous malformations: evaluation by single-photon emission CT. *AJNR* **1987**;8:193–197
9. Jinkins JR. Encephalopathic cerebrovascular steal: dynamic CT of arteriovenous malformations. *Neuroradiology* **1988**;30:201–210
10. Marks MP, O'Donohue J, Fabricant JI, et al. Cerebral blood flow evaluation of arteriovenous malformations with stable xenon CT. *AJNR* **1988**;9:1169–1175
11. Marks MP, Lane B, Steinberg G, Chang P. Angiographic determinants of hemorrhage in intracerebral arteriovenous malformations. *Radiology* **1990**;176:807–813
12. McCormick WF. Pathology of vascular malformations of the brain. In: Wilson CB, Stein BM, eds. *Intracranial arteriovenous malformations*, 1st ed. Baltimore: Williams & Wilkins, **1984**:44–63
13. Marks MP, DeLaPaz RL, Fabrikant JI, et al. Intracranial vascular malformations: imaging of charged-particle radiosurgery. Part I. Results of therapy. *Radiology* **1988**;168:447–455
14. Fleis J. *Statistical methods for rates and proportions*, 2nd ed. New York: Wiley, **1981**:25–27
15. Feindel W, Perot P. Red cerebral veins: a report on arteriovenous shunts in tumors and cerebral scars. *J Neurosurg* **1965**;22:315–325
16. Norlen G. Arteriovenous aneurysms of the brain. Report of 10 cases of total removal of the lesion. *J Neurosurg* **1949**;6:475–494
17. Carrasco-Zanini J. Arteriovenous malformations of the brain and their effect on cerebral vessels. *J Neurol Neurosurg Psychiatry* **1957**;20:241–249
18. French LA, Chou SN. Conventional methods of treating intracranial arteriovenous malformations. *Prog Neurosurg* **1969**;3:274–319
19. Prosenz P, Heiss W, Kvicala V, Tschabitscher H. Contribution to the hemodynamics of arterial venous malformations. *Stroke* **1971**;2:279–289
20. Lassen NA, Munck O. Cerebral blood flow in arteriovenous anomalies of the brain determined by the use of radioactive krypton 85. *Acta Psychiatr Scand* **1956**;31:71–80
21. Haggendal E, Ingvar DH, Lassen NA, et al. Pre- and posteroperative measurements of regional cerebral blood flow in three cases of intracranial arteriovenous aneurysms. *J Neurosurg* **1965**;22:1–6
22. Homan RW, Devous MD, Sokly EM, Bonte FJ. Quantification of intracerebral steal in patients with arteriovenous malformation. *Arch Neurol* **1986**;43:779–785
23. Batjer HH, Devous MD, Seibert GB, et al. Intracranial arteriovenous malformation: relationships between clinical and radiographic factors and ipsilateral steal severity. *Neurosurgery* **1988**;23:322–328
24. Duvernoy HM, Delon S, Vannson JL. Cortical blood vessels of the human brain. *Brain Res Bull* **1981**;7:519–579
25. Tatelman M. Pathways of cerebral collateral circulation. *Radiology* **1960**;75:349–362
26. Hawkins TD. The collateral anastomoses in cerebro-vascular occlusion. *Clin Radiol* **1966**;17:203–219
27. Hinshaw DB, Thompson JR, Hasso AN. Adult arteriosclerotic moyamoya. *Radiology* **1976**;118:633–636
28. Nornes H, Grip A. Hemodynamic aspects of cerebral arteriovenous malformations. *J Neurosurg* **1980**;53:456–464
29. Hassler W. Hemodynamic aspects of cerebral angiomas. *Acta Neurochir* (Wien) **1986**;S37:1–136
30. Pile-Spellman JMD, Baker KF, Liszczak TM, et al. High-flow angiopathy: cerebral blood vessel changes in experimental chronic arteriovenous fistula. *AJNR* **1986**;7:811–815
31. Mawad ME, Hilal SK, Michelsen WJ, Stein B, Ganti SR. Occlusive vascular disease associated with cerebral arteriovenous malformations. *Radiology* **1984**;153:401–408
32. Omojola MF, Fox AJ, Vinuela F, Debrun G. Stenosis of afferent vessels of intracranial arteriovenous malformations. *AJNR* **1985**;6:791–793
33. Abe M, Kjelberg RN, Adams RD. Clinical presentations of vascular malformations of the brain stem: comparisons of angiographically positive and negative types. *J Neurol Neurosurg Psychiatry* **1989**;52:167–175